DD

KEK P 93-129
SW 9405

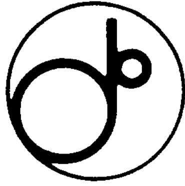

KEK Preprint 93-129
HUPD 9323
OUHEP 93-3
October 1993
H

Micro-Discharges of AC-Coupled Silicon Strip Sensors

T. OHSUGI, Y. IWATA, H. OHYAMA, T. OHMOTO, M. OKADA, M. YOSHIKAWA,
N. TAMURA, T. HATAKENAKA, Y. UNNO, T. KOHRIKI, N. UJIIE, H. MIYATA, T. ASO,
R. TAKASHIMA, A. MURAKAMI, S. KOBAYASHI, K. YAMAMOTO,
K. YAMAMURA and M. MURAMATSU

CERN LIBRARIES, GENEVA

P00020291

Presented at the International Symposium on
Development and Application of Semiconductor Tracking Detectors
May 22-24, 1993, Hiroshima, Japan

National Laboratory for High Energy Physics, 1993

KEK Reports are available from:

Technical Information & Library
National Laboratory for High Energy Physics
1-1 Oho, Tsukuba-shi
Ibaraki-ken, 305
JAPAN

Phone: 0298-64-1171
Telex: 3652-534 (Domestic)
(0)3652-534 (International)
Fax: 0298-64-4604
Cable: KEK OHO
E-mail: LIBRARY@JPNKEKVX (Bitnet Address)
library@kekvax.kek.jp (Internet Address)

Micro-Discharges of AC-Coupled Silicon Strip Sensors

T. Ohsugi, Y. Iwata, H. Ohyama, T. Ohmoto, M. Okada and M. Yoshikawa
Department of Physics, Hiroshima University, Higashi-Hiroshima 724, Japan

N. Tamura and T. Hatakenaka
Department of Physics, Okayama University, Okayama 700, Japan

Y. Unno, T. Kohriki and N. Ujiie
National Laboratory for High Energy Physics, KEK, Tsukuba 305, Japan

H. Miyata and T. Aso
Department of Physics, Niigata University, Niigata 950-21, Japan

R. Takashima, Kyoto University of Education, Kyoto 612, Japan

A. Murakami and S. Kobayashi,
Department of Physics, Saga University, Saga 840, Japan

K. Yamamoto, K. Yamamura and M. Muramatsu
Hamamatsu Photonics Co., Hamamatsu 435, Japan

Abstract

Micro-discharge at the edges of strips in AC-coupled silicon strip sensors has been investigated. A steep increase in the leakage current (breakdown) and a sudden onset of burst noise were observed at a low reverse-bias voltage when the bias potential was across the AC-coupling capacitor. This can be explained by the occurrence of micro-discharges along the edges of strips. These discharges have been confirmed by observing IR light emission. A calculation of the field strength at the strip edge suggests that a fringe field of the external electrode generates the micro-discharge at the strip edge when the bias voltage is 50 ~ 80 V. This is consistent with our observations. We discuss a design for AC-coupled sensors that eliminates this discharge problem.

Introduction

Robust and reliable AC-coupled double-sided microstrip sensors are required for tracking detectors which will be used in high-energy and high-intensity beam experiments in the next generation of accelerators, such as the SSC and the LHC. An AC-coupled readout is of essential importance to reduce the impact of dark current increase arising from radiation damage. A double-sided readout is also required to reduce the material thickness and to attain a good tracking capability for electrons and low-momentum particles. The coupling capacitor of a double-sided detector should hold the full bias potential. For a single-sided sensor, the strips of the readout side can be grounded and the positive bias applied to the other side. The potential difference between the electrodes of the coupling capacitor is then small, equal to or less than 10 V. On the other hand, for a double-sided sensor, the coupling capacitors on one or both sides must hold or share the full bias potential without any breakdown. Since the intrinsic breakdown voltage of SiO_2 is high enough to hold 200 V for 0.2 μm thickness (we assume an ideal SiO_2), the breakdown of the coupling capacitor itself is not at issue here. The large potential difference between the external electrode and the implanted strip results in a strong fringe field at the edge of the strip, inside of the silicon substrate (MOS effect). This causes micro-discharges due to the high local field strength, at a voltage which is considerably lower than the breakdown voltage of the corresponding DC-coupled sensor. We now discuss the properties of this micro-discharge effect in AC-coupled microstrip sensors, and propose a treatment of the problem.

Experimental observation

The microstrip sensors used for the following observation were all single-sided and AC-coupled. They were fabricated with n-type substrates of 4 ~ 8 kΩ·cm resistivity. The strip pitch was either 50 or 100 μm.

At first, by observing the leakage current, we determined that junction breakdown did not occur for bias voltages up to 150 V in either the p^+ or n^+ strip sensors when the external electrode was left floating. In other words, up to 150 V, no junction breakdown was observed when there was no potential difference between the two electrodes of the coupling capacitor. The leakage current showed a clear plateau, as in case of a reverse-biased diode. On the other hand, when the bias potential was across the AC-coupling capacitor, a sharp increase in the leakage current (breakdown) was observed at a bias voltage of around 65 V for the p^+ strip sensor (Fig. 1). This was not catastrophic, but rather reversible and reproducible phenomenon. After the sharp increase, the leakage current saturated and again showed a plateau. A similar phenomenon was observed with the n^+ strip sensor, but the onset voltage of breakdown was higher by ~ 30 V than that for the p^+ strip sensor. These breakdowns are similar to the edge-type breakdown discussed by Longoni et al.[1], but occur at a significantly lower voltage.

Large-amplitude noise (burst noise) appeared when we measured the signal amplitude as a function of the bias voltage. In this case the negative bias potential was supplied to the p^+ strips so that the full potential was held by the coupling capacitor. Figure 2 shows the root-mean-square (rms) noise amplitude of the p^+ strip sensor as a function of the bias

voltage. The noise pulses were generated randomly and the amplitude increases sharply as the bias voltage increased. The threshold voltage at which this sharp increase occurred was the same as that for the leakage current. These effects were observed in a sensor in which the external electrode and the implanted p+ strip were of equal width. The amplifier system used in this measurement was a combination of a charge amplifier and a spectroscopy amplifier with a 0.5 μs shaping time.

Temperature dependence

The temperature dependence of the burst noise generation (breakdown) is shown in Fig. 3. A positive temperature coefficient can be clearly seen; that is, the breakdown voltage increases with increasing temperature. The positive temperature coefficient suggests that this is an avalanche-type breakdown.[2]

Calculation of the field strength

The electric field in the region of the implanted strip was calculated for the simplified geometry of the implant and the external electrode, assuming -65 V on the implant and a grounded external electrode. A positive charge in the Silicon-SiO_2 interface accumulated by irradiation was not taken into account in this calculation. However, the maximum effect of the charge can be estimated from the switching voltage shift of the MOSFET [3] to be the equivalent potential of about -20 V addition to the bias. For the purpose of the calculation we assumed a 1μm thick implanted, 1μm thick external electrode, both with sharp rectangular boundaries, and a 0.2 μm thick SiO_2 coupling insulator between them. Several geometries were tried, varying

the relative position of the edge of the external electrode and the edge of the implant. Figure 4 demonstrates the equipotential lines calculated around the implant and the external electrode for the geometries of which the edge of the external electrode is placed just above the edge of the implant (4-a) and the edge of the external electrode stepped back by 1 μm (4-b). In each case the highest field strength in the silicon bulk is calculated and plotted in Fig. 5 as a function of the edge separations. The breakdown field of silicon is approximately 30 V/μm [4], which coincides with the edge field strength calculated at the edge of the p^+ implant for the case in which the edge of the external electrode is placed just above the edge of the implant. This calculation suggests that the external electrode must be placed inside from the edge of the implant by 1 ~ 2 μm in order to avoid the breakdown at the edge of the implant. We note that the actual boundary of the implant is rounded off by diffusion. This doesn't help, in this case, to reduce the highest field strength around the implant, since the highest field point is at the corner facing the SiO_2 insulator.

Test samples and measurements

To examine the calculated results, we fabricated test samples which had the external electrode having four different geometries, as shown in Fig. 6-a. All of the samples are single-sided, AC-coupled p^+ strip sensors. The width of the implanted p^+ strip was 12 μm for all of the strips, while the external electrodes were four different widths of 4, 6, 8 and 16 μm. The coupling insulator was 0.22 μm thick SiO_2. The bias feeding resistors were made with polycrystalline silicon. The bonding

pads were installed inside the bias/guard ring. To avoid the micro-discharges around the bonding pad area, the p^+ implant was made wider than the bonding pad, thereby covering the entire region of the pad (Fig. 6-b). Contact pads only for the external electrodes were installed and no DC contact pads for the implant in these samples. Consequently, the leakage current of each strip could not be measured.

The rms amplitude of noise measured as a function of the bias voltage for each of the four geometries is presented in Fig. 7. The bias potential was applied for this measurement so that the potential was across the AC-coupling capacitor. The breakdown voltage varies with the four widths of the external electrode. The 16 μm external electrode overhangs 2 μm from the implant edge. The burst noise of this sample starts at the bias of 55 V, which is clearly lower than the onset voltage of 65 V in the case of which the edge of the external electrode is placed just on the edge of the implant. The edges of 8 and 6 μm electrodes are stepped back by 2 and 3 μm from the edge of the implant and the onset voltages of around 90 and 120 V, respectively. These observations are qualitatively consistent with the calculation mentioned above. No clear difference between the 4 and 6 μm wide electrodes can be found. This is because the 6 μm electrode is sufficiently narrow to reduce the field strength at the edge, and further stepping back of the edge by 1 μm has no appreciable effect, as suggested from the calculation. It should be noted that a ± 1 μm placement error between the implant and the external electrode might reduce the effect of geometry difference.

Infrared light emission

To observe direct evidence of the micro-discharges at the edge of the implant due to the MOS effect, we fabricated special sensors having the external electrode made with polycrystalline silicon (poly-Si) instead of aluminum. The IR lights which were emitted at the strip edge by the micro-discharges were observed through the thin, poly-Si electrode by a high sensitive CCD camera.[5] The growing edge of the strip can be clearly seen as a brightly colored edge in the picture of Fig. 8. The bias potential was applied to the p-strip and the external electrode of the center strip was grounded so that full potential was across the integrated capacitor. On the other hand, adjacent electrodes on both sides were floating.

Discussions

The steep increase in the leakage current and the sharp increase in the noise amplitude (burst noise) for the AC-coupled sensors can be explained by the occurrence of the micro-discharge (avalanche breakdown) at the edge of the implant due to the MOS effect. This explanation is supported by the temperature dependence of the breakdown curve as well as observations of the IR light emission. The micro-discharge is a phenomenon similar to that caused by the edge instability discussed by Longoni [1] at a higher bias voltage. However, the micro-discharge due to the MOS effect takes place at a much lower voltage and is strongly dependent on the relative geometry between the edge of external electrode and the edge of the implant. For the overhanging geometry of the external electrode, the micro-discharge starts at about 55 V, while the external

electrode being placed 2 μm or more stepping back from the edge of the implant improves the onset voltage of breakdown up to the bias voltage of 120 V.

Even at the edge of the n^+ strip the micro-discharges due to the MOS effect will take place if the edge field is sufficiently high due to a large potential difference between the n^+ strip and the external electrode, though there is no junction at the surface of the n^+ strip. However, we can expect an extra margin of 20 ~ 40 V for the onset voltage of the n^+ strip, because the positive charge accumulated in the SiO_2 insulator during the process or by the ionizing irradiation works in an opposite way in comparison with the p^+ strip side.

Conclusions

The coupling capacitor of the double-sided strip sensor should hold a potential applied as a bias. Then, the MOS effect causes the micro-discharges at the edge of the implant at a rather lower voltage such as 55 ~ 70 V.

This micro-discharges problem due to the MOS effect can be significantly improved by an elaborate design of the external electrode for the AC-coupled sensor. The external electrode should be placed inside by 2 ~ 3 μm (including 1 μm placing error) from the edge of the implanted strip in order to reduce the field strength at the edge. Then, the onset voltage of the micro-discharge improves from 60 to 120 V.

The positive charge at the interface of SiO_2 and silicon bulk accumulated by irradiation lowers the onset voltage of the micro-discharge (breakdown) at the p^+ strip, while the at the n^+ strip it pushes up the onset voltage. The amount of the

accumulated charge is sensitive to insulator material, structure, and fabrication process. A systematic study of ionization radiation effects on the micro-discharge is necessary for the design of a reliable radiation-hard AC-coupled microstrip sensor.

Acknowledgments

We would like to express our thanks to the Japanese members of the SDC group for their encouragement during this study. Also, many thanks are due to the members of the silicon subgroup of the SDC for their valuable discussions and kind suggestions.

This study was partially supported by the Japan-US cooperation in the field of High Energy Physics, and also partially supported by the Joint Research in International Scientific Research Program, Ministry of Education, Culture and Science, Japan.

References

[1] A. Longoni, M. Sampietro and L. Struder, Nucl. Instr. and Methods, A288 (1990) 35.

[2] S.M. Sze, Physics of Semiconductor Devices, JOHN WILEY & SONS, New York, 1981, p98.

[3] T.P. Ma and P.V. Dressendorfer, IONIZING RADIATION EFFECTS IN MOS DEVICES AND CIRCUITS, JOHN WILEY & SONS, New York, 1989, N. Bacchetta et al., Nucl. Instr. and Meth, A326 (1993) 381.

[4] S.M. Sze, Physics of Semiconductor Devices, JOHN WILEY & SONS, New York, 1981, p 850.

[5] Hot electron analyzer PHEMOS-50, Hamamatsu Photonics

Figure captions

Fig. 1. Leakage current as a function of the bias voltage when the potential is across the integrated capacitor on the p-strip.

Fig. 2. Rms amplitude of the burst noise as a function of the bias voltage when the potential is across the integrated capacitor on the p-strip.

Fig. 3. Temperature dependence of the rms amplitude of the burst noise.

Fig. 4. Equipotential lines calculated around the edge of the implant and the external electrode. Figure 4-a is for the geometry of the edge of the external electrode placed just on the edge of the implant. Figure 4-b is for the geometry of the edge of the external electrode stepped back by 1 μm from the edge of the implant.

Fig. 5. The Highest field strength calculated at around the implant is plotted as a function of the edge separation of the external electrode and the implant. The positive value of the horizontal axis means that the external electrode overhangs on the implant.

Fig. 6. Schematic pictures of the samples for examining the micro-discharges at the edge of the implant. Figure 6-a indicates the configuration of the four types of external electrode tested. Figure 6-b shows the geometry of the bonding pad area.

Fig. 7. Rms amplitude of the burst noise shown as a function of the bias voltage for each geometry taken from the test samples.

Fig. 8. Bright color indicates the IR light emission by the micro-discharges. The external electrode of the center strip is grounded, while the others are floating.

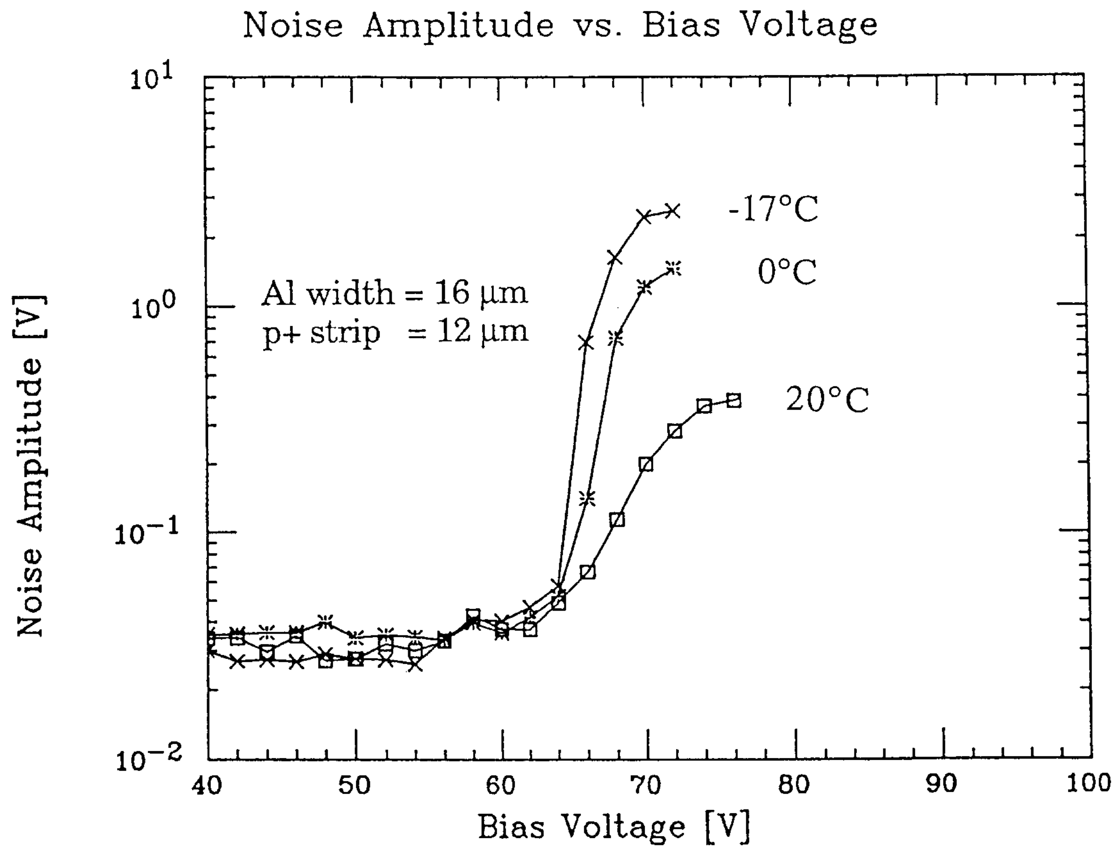

Fig. 3

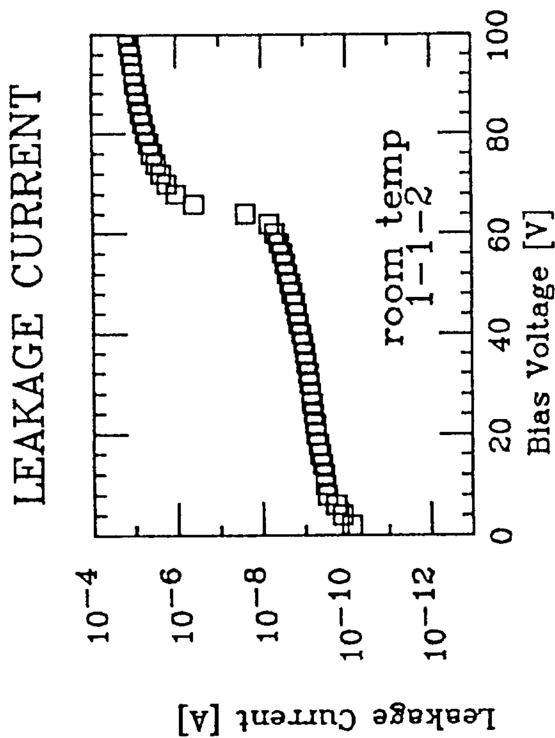

Fig. 1

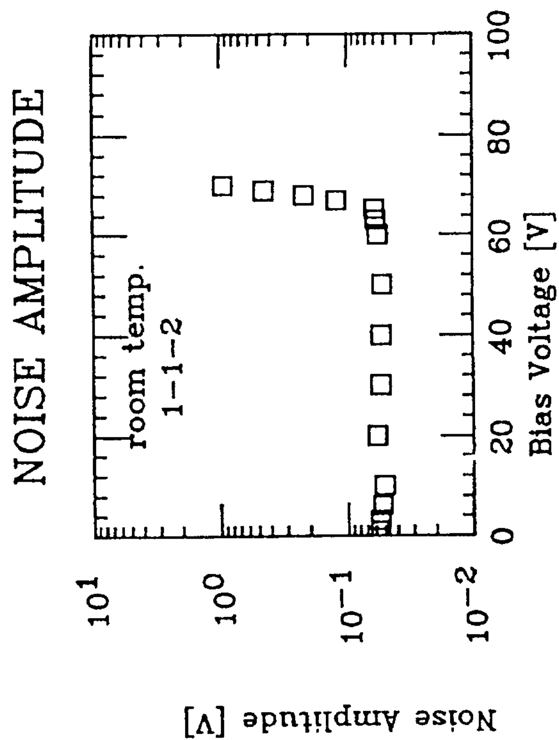

Fig. 2

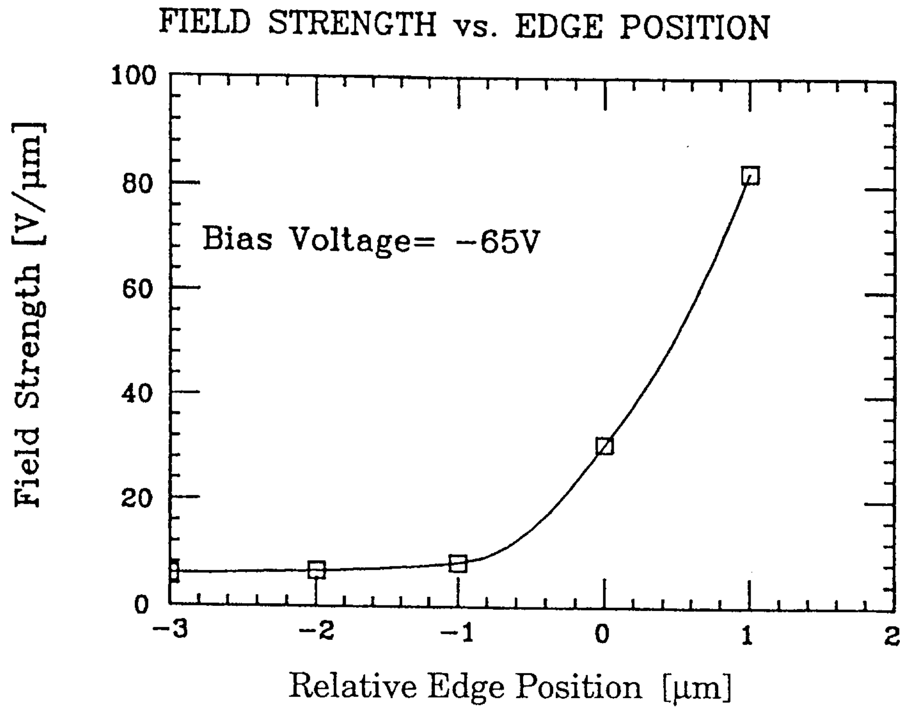

Fig. 5

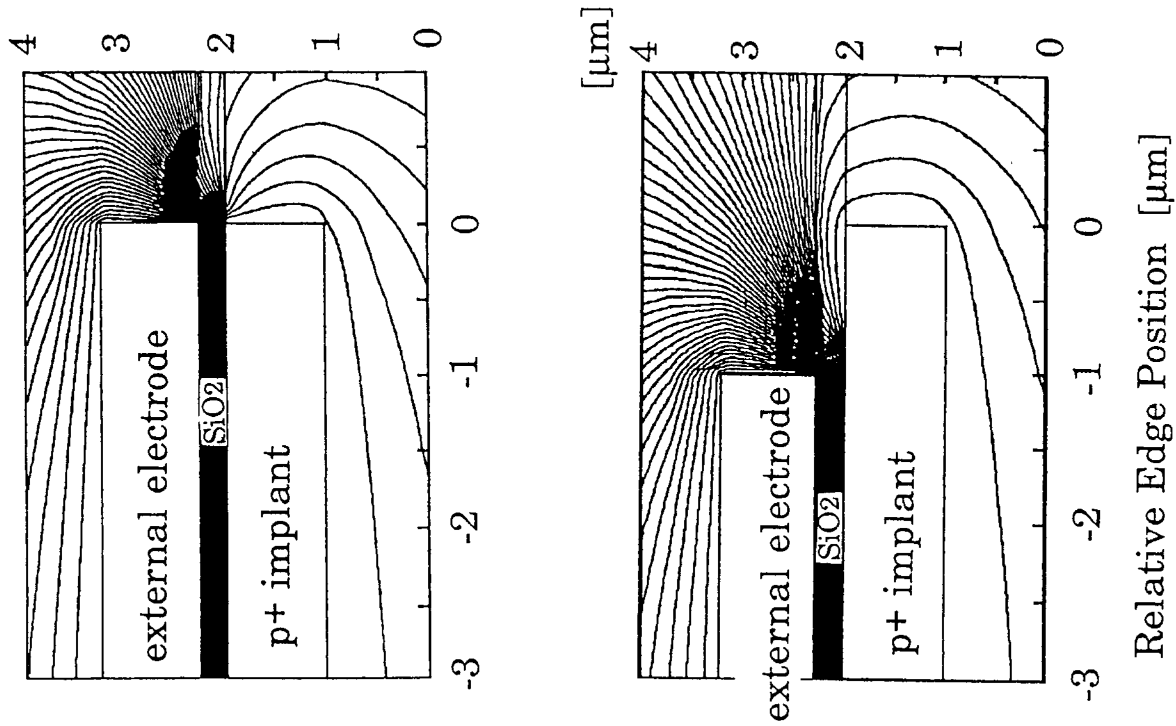

Fig. 4

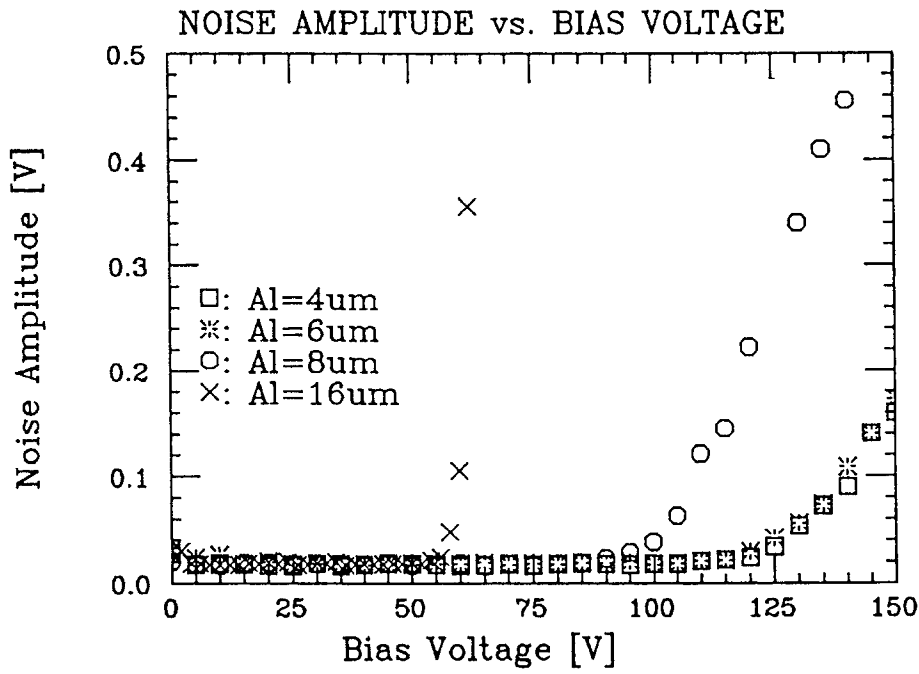

Fig. 7

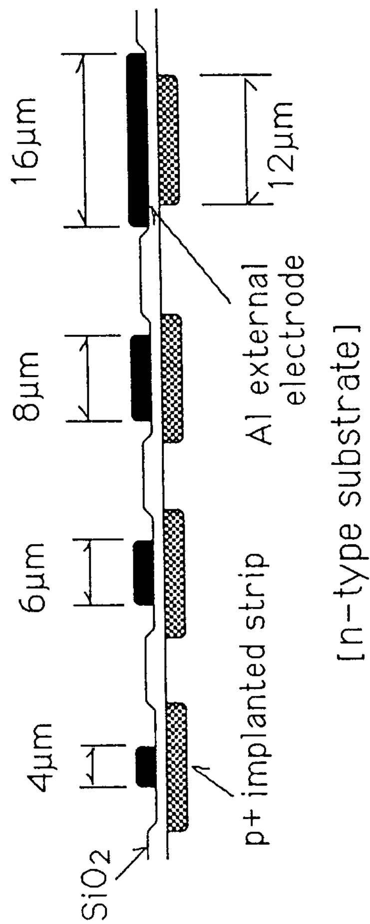

Fig. 6 (a)

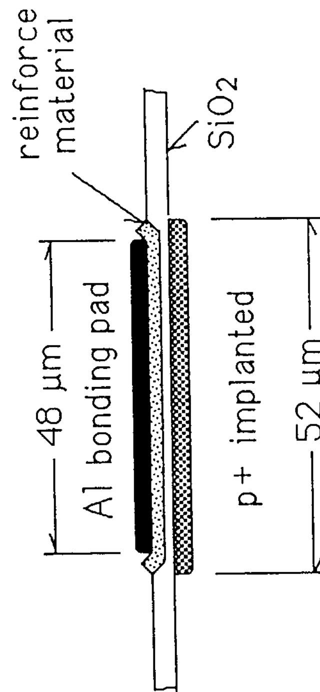

Fig. 6 (b)

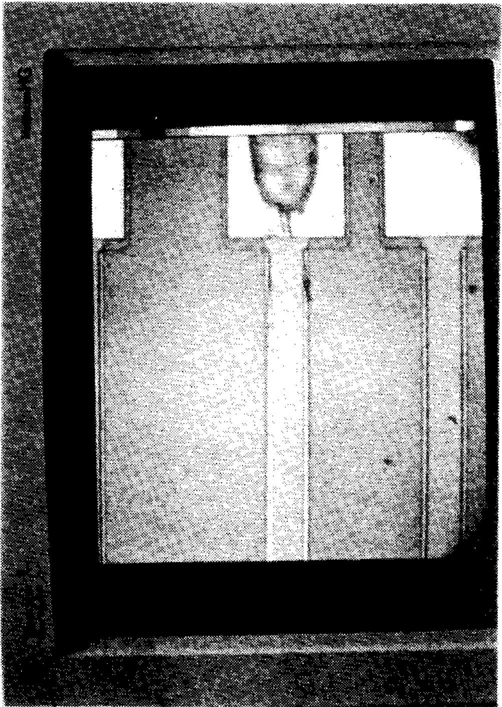

Fig. 8